Multi-feature Clustering of Step Data using Multivariate Functional Principal Component Analysis

WOOKYEONG SONG AND HEE-SEOK OH
Seoul National University
Seoul 08826, Korea

YAEJI LIM Chung-Ang University Seoul 06974, Korea

YING KUEN CHEUNG Columbia University New York 10032, USA

Draft: version of October 16, 2020

Abstract

This paper presents a new statistical method for clustering step data, a popular form of health record data easily obtained from wearable devices. Since step data are high-dimensional and zero-inflated, classical methods such as K-means and partitioning around medoid (PAM) cannot be applied directly. The proposed method is a novel combination of newly constructed variables that reflect the inherent features of step data, such as quantity, strength, and pattern, and a multivariate functional principal component analysis that can integrate all the features of the step data for clustering. The proposed method is implemented by applying a conventional clustering method such as K-means and PAM to the multivariate functional principal component scores obtained from these variables. Simulation studies and real data analysis demonstrate significant improvement in clustering quality.

Keywords: Functional data; K-means; Multivariate functional principal component analysis; PAM; Step data.

1 Introduction

Along with a growing interest in digital and smart healthcare, studies of physical activity measured using wearable devices are also on the rise. Analysis of personal health record data can provide a concise and meaningful insight into an individual's state of activity, enabling them to provide customized health care services based on personalized data. Le Masurier et al. (2005) used pedometers to determine the physical activity levels of American youth. Bassett et al. (2010) analyzed the number of daily steps in various demographic subgroups to identify predictors of pedometer-measured physical activity performed by American adults. In recent years, statistical learning methods have used for activity recognition studies. Shoaib et al. (2015) studied the clustering of living activities by analyzing data from smartphones and smartwatches based on a support vector machine and decision trees. Balli et al. (2005) compared the naive Bayes, k-nearest-neighbors, logistic regression, Bayesian network, and multilayer perceptron methods in terms of human activity recognition using smartwatch sensor data.

This study analyzes step count data recorded from a wearable device, *Fitbit*, that tracks the wearer's activity. Data used for the analysis are recorded for 21,394 days for 79 users and are collected at one-minute intervals, yielding 1440 epochs per day per individual. In this paper, we want to cluster "days" based on physical activity information.

We propose a new clustering method that reflects the vital intraday characteristics of physical activities such as amount, intensity, and pattern. The proposed method consists of two key elements: the composition of new functional variables and a multivariate functional principal component analysis (MFPCA). The construction of the new variables is designed to represent the step data's inherent features, such as quantity, strength, and pattern. The MFPCA applied to the new variables provides low-dimensional MFPC scores so that some conventional clustering methods can be used to the step data analysis. Specifically, we first generate new variables and apply the MFPCA to the new variables. Classical clustering methods such as K-means or partitioning around medoids (PAM) (Kaufman and Rousseeuw, 1987) are then applied to low-dimensional MFPC scores.

In the literature, there are numerous clustering methods for multivariate functional data. Jacques and Preda (2014) presented a parametric mixture model for multivariate functional data, which uses the multivariate probability density of the principal component vector as a proxy for the density of the original data. Chiou et al. (2014) investigated a normalized MFPCA and its application to functional clustering. Bouveyron et al. (2016) proposed a discriminative functional mixture (DFM) model that models data into one distinct functional subspace. The FunFEM algorithm was further proposed for inference using the DFM model. Schmutz et al. (2020) suggested clustering multivariate functional data by projecting data into low-dimensional subspaces using an MFPCA and a functional latent mixture model. We emphasize that the proposed method fully reflects the crucial features of step data: discrete (count), high-dimensional, and zero-inflated, which is the crucial contribution that distinguishes the proposed method from the existing methods.

In our previous work, Lim et al. (2019) introduced input variables for clustering accelerometer data based on a rank-based transformation and thick-pen transformation. The main difference is that the proposed method in this article considers the amount, intensity, and pattern of the step count data simultaneously for clustering, while Lim et al. (2019) considered the amount and pattern of activity separately. This is a critical extension as daily step data is a complex process defined by more one single feature such as amount and pattern. Also importantly, the proposed method is applicable to discrete and zero-inflated data, which are natural attributes of step data. This is also a significant improvement of the existing clustering approaches.

The rest of this paper is organized as follows. Section 2 presents the scheme of constructing new variables. In Section 3, the proposed clustering method based on MFPCA and the constructed variables is proposed. Section 4 discusses real data analysis with having the step count data, and Section 5 further performs simulation studies with various test functions beyond step count data to assess the effectiveness of a general clustering method. Concluding remarks are provided in Section 6.

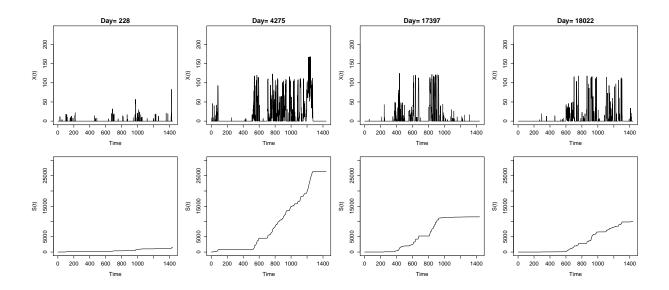


Figure 1: Four step count datasets X(t) according to four different days (top row), and the corresponding cumulative sum functions S(t) (bottom row).

2 Construction of Multiple Functional Input Variables

This section introduces three variables generated from the original step data X(t), t = 1, ..., T, i.e., the amount, intensity, and pattern of physical activity.

2.1 Cumulative Sum Function

For a given real-valued process $\{X(t): t \in (0,T)\}$, the cumulative activity up to t is defined as $S(t) := \int_0^t X(u) du$, $t \in (0,T)$. Since the cumulative sum represents the amount of the activity in the step data, S(t) is considered as a functional variable, termed *cumulative sum function*.

Figure 1 shows the original step datasets X(t), and the corresponding cumulative sum functions S(t) over the four randomly selected days. By comparing the cumulative sum functions, it can identify the quantity of daily activity. On day 4275, a large amount of activity is observed compared to 228, 17397, and 18022 days. However, focusing on the amount of information in the data may not reflect some vital features like time-related information, such as activity intensity or pattern. For example, the cumulative totals of days 17397 and 18022 seem similar, but these original step data have different patterns.

2.2 Ordered Quantile Slope Function

The intensity of the step data can be useful for understanding and classifying an individual's state of activity beyond the simple total steps of the data. To this end, a quantile-based function is considered to reflect the intensity of step data (Cheung et al., 2018). We first define the 100pth quantile of the activity time as

$$\mathcal{T}(p) := \inf\{t | S(t) \ge pS(T)\},\tag{1}$$

where $S(t) = \int_0^t X(u) du$ as defined in Section 2.1. $\mathcal{T}(p)$ can be interpreted as the time when the 100p percent of the total activity has been achieved. For example, $\mathcal{T}(0.5)$ indicates the time to reach the middle activity of the day. A quantile slope function between $\mathcal{T}(p_q)$ and $\mathcal{T}(p_{q+1})$ is then defined as

$$s(t) := \frac{S(T)/Q}{\mathcal{T}(p_{q+1}) - \mathcal{T}(p_q)}, \quad \text{for} \quad \mathcal{T}(p_q) \le t < \mathcal{T}(p_{q+1}),$$

where $p_q = \frac{q}{Q}$, q = 0, ..., Q and Q is the number of quantiles. The quantile slope function s(t) provides the intensity of the activity, which shows how long it takes to achieve $\frac{1}{Q}$ of the total number of steps per day. Figure 2(a) and (b) show the step data, X(t) for a particular day and the corresponding cumulative function, S(t). In the figure, the red vertical lines indicate quantiles, $\mathcal{T}(p_q)$, where $p_q = \frac{q}{4}$ (q = 0, ..., 4). The quantiles $\mathcal{T}(p_q)$ seem to detect the high intensity time points well. In addition, the corresponding quantile slope function s(t) is plotted in Figure 2(c), which shows the slope information in S(t) clearly.

To examine the intensity of the activity further, we eliminate the time information of s(t) by ordering it,

$$I_Q(t) := s_{(t)}, \quad t = 1, 2, \dots, T,$$

where $s_{(t)}$ is the smallest value of s(t). $I_Q(t)$ is termed ordered quantile slope function of X(t) with Q quantiles. Figure 2(d) shows $I_Q(t)$ of step data X(t), and Figure 3 shows $I_Q(t)$'s from four randomly selected days. As one can see, the number of step counts on day 17439 is tiny, except near t = 500, where a spike in the number of steps occurred. Likewise, on day 3713, the surge in activity is about

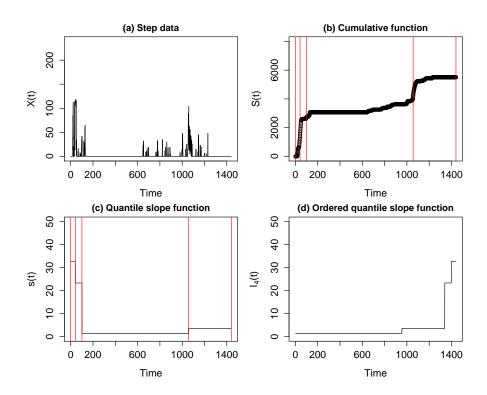


Figure 2: (a) Step data X(t) in day 20682, (b) the corresponding cumulative function S(t), (c) quantile slope function s(t), and (d) ordered quantile slope function $I_Q(t)$. Note that the red vertical lines indicate quantiles $\mathcal{T}(p_q)$.

t=1340. The ordered quantile slope function $I_Q(t)$ shows such intensity at a high peak close to t=1440. Meanwhile, the activity on day 813 is concentrated between t=1000 and t=1250 but is not as intense as that on days 17439 and 3713. Therefore, $I_Q(t)$ on day 813 is much lower than that on days 17439 and 3713.

To assess the effect of the number of quantiles Q, we compute S(t) and $I_Q(t)$ on day 20684 for different values of Q = 3, 6, 12, 18. As shown in Figure 4, the S(t) detects the moderate-intensity from t = 600 to 1250 for all Q's. The magnitude of $I_Q(t)$ changes with an increase of Q. A small Q makes it difficult to detect intensity information, while a large Q makes the calculation time long. For the real data analysis and simulation study, we set Q = 8, and the sensitivity test presented in Section 4.3 ensures that the clustering result is robust to the choice of Q value.

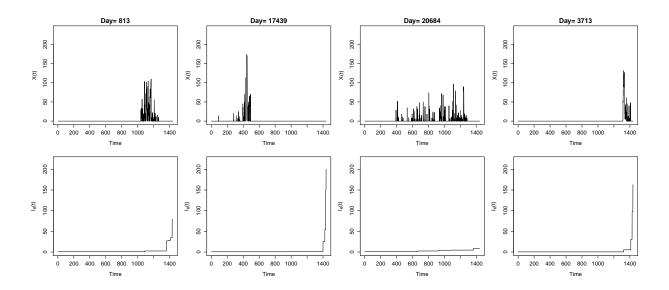


Figure 3: Four step datasets X(t) (top row), and the corresponding ordered quantile slope functions $I_Q(t)$ with Q=6 (bottom row).

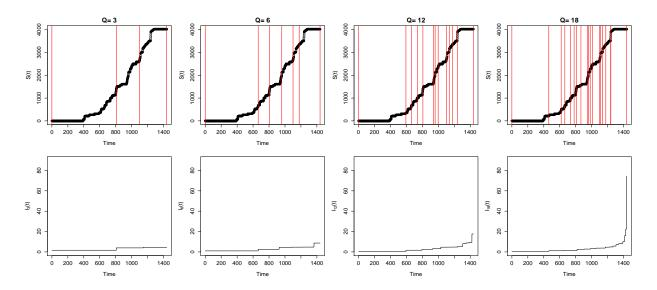


Figure 4: Cumulative sum functions S(t) for a specific day with $\mathcal{T}(p_0), \dots, \mathcal{T}(p_Q)$ with Q = 3, 6, 12, 18, marked by red vertical lines (top row), and the corresponding quantile slope functions $I_Q(t)$ (bottom row).

2.3 Mean Score Function

We consider a new variable to reflect the pattern of physical activity. We first define the cumulative sum of ordered steps as $S_{(t)} := \int_0^t X_{(u)} du$ for $t \in (0, T)$, where $X_{(t)}$ denotes the tth smallest value of $\{X(t)\}_{t=1}^T$. In a similar way to the $\mathcal{T}(p)$ defined in (1), we define the 100pth quantile of the ordered activity time as

$$\mathcal{T}_{(p)} := \inf\{t | S_{(t)} \ge p S_{(T)}\},\$$

which indicates the time when the step data reordered in ascending order achieved 100p of the total activity. Then, we define the score function u(t) as

$$u(t) = q$$
, if $\mathcal{T}_{(p_q)} < \operatorname{rank}(X_{(t)}) \le \mathcal{T}_{(p_{q+1})}$,

where $p_q = \frac{q}{Q}$, q = 0, ..., Q. Thus, the u(t) represents the activity at time t compared to that at other time points. For further examining the pattern of the activity, we compute the local average of u(t), termed mean score function via quantile of ordered data $X_{(t)}$ with Q + 1 quantiles,

$$P_Q(t) := \begin{cases} \frac{1}{T/Q} \sum_{k=1}^{t_1} u(k), & \text{for } 0 < t \le t_1 \\ \frac{1}{T/Q} \sum_{k=t_1+1}^{t_2} u(k), & \text{for } t_1 < t \le t_2 \\ & \vdots \\ \frac{1}{T/Q} \sum_{k=t_{Q-1}+1}^{T} u(k), & \text{for } t_{Q-1} < t \le T, \end{cases}$$

where $t_q = T \times p_q$, q = 1, ..., Q - 1. To identify both global and local patterns of the activity, we use the local average of u(t) rather than itself. Figure 5 shows the mean score function $P_Q(t)$ with Q = 4 for four randomly selected days. We observe that $P_Q(t)$ represents the pattern of the step data, whereas the information of the amount and intensity has disappeared. For example, on day 6042, most activities occur between t = 600 and t = 800 and are well reflected in the corresponding mean score function. Also, on day 1276, activities are evenly distributed from t = 400 to t = 1100, which can be observed from the mean score function.

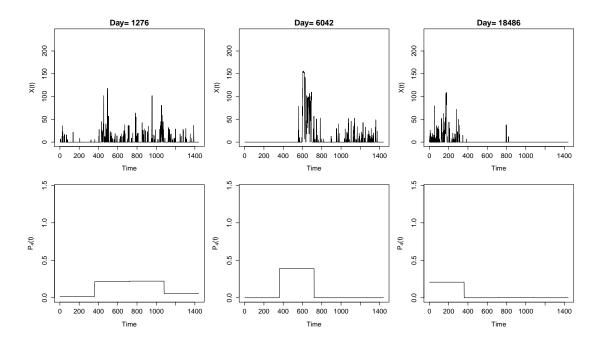


Figure 5: Three step datasets X(t) (top row), and the corresponding mean score functions $P_Q(t)$ with Q=4 (bottom row).

3 Proposed Method for Clustering

This section proposes a clustering procedure using the variables defined in Section 2. For this purpose, we represent the variables defined in Section 2 as continuous functional data on a finite-dimensional space spanned by basis functions. Let $X_i(t) := (X_{1i}(t), X_{2i}(t), X_{3i}(t))^T$ for i = 1, 2, ..., N, t = 1, ..., T, where

- $X_{1i}(t)$ functional data of the cumulative sum function, $S_i(t)$.
- $X_{2i}(t)$ functional data of the ordered quantile slope function, $I_{Q_1,i}(t)$.
- $X_{3i}(t)$ functional data of the mean score function via quantile of ordered data, $P_{Q_2,i}(t)$.

Here Q_1 and Q_2 are the predetermined numbers of quantiles used in the ordered quantile slope function and mean score function, respectively. Thus, $X_i(t)$ are multi-feature functional data that reflect the quantity, intensity, and pattern of the step counts in the *i*th day. For our analysis, we standardize the kth variable as

$$Z_{ki}(t) := \frac{X_{ki}(t)}{\left(\frac{1}{N} \sum_{i=1}^{N} \max_{t=1,\dots,T} X_{ki}(t)\right)}, \quad i = 1, 2, \dots, N, \ k = 1, 2, 3.$$

Then $Z_{ki}(t)$ is represented as $Z_{ki}(t) = \sum_{r=1}^{R_k} c_{kir} \phi_{kr}(t)$, $k = 1, 2, 3, 0 \le t \le T$, where $\phi_{kr}(t)$ is the basis function for the kth variable, and R_k is the number of basis functions. In this study, we use a B-spline basis with a cubic polynomial segment (de Boor, 1978).

We now perform a clustering procedure by applying an MFPCA to the standardized functional data $\mathbf{Z}_i(t) := (Z_{1i}(t), Z_{2i}(t), Z_{3i}(t))^T$. For a self-contained material, we briefly review the MFPCA. Suppose that we have $\mathbf{Z}(t) := (Z_1(t), Z_2(t), \dots, Z_p(t))^T$, $t \in \mathcal{T}$, in a Hilbert space of p-dimensional functions in $L_2(\mathcal{T})$, denoted by \mathbb{H} . Let $\boldsymbol{\mu}(t) = (\mu_1(t), \dots, \mu_p(t))$, where $\mu_k(t) = E(Z_k(t))$, $k = 1, \dots, p$, denotes the continuous mean function, and $\boldsymbol{V}(s,t) = \mathbb{E}[(\boldsymbol{Z}(s) - \boldsymbol{\mu}(s)) \otimes (\boldsymbol{Z}(t) - \boldsymbol{\mu}(t))]$, $s,t \in \mathcal{T}$, denotes the covariance matrix. The inner product is defined as

$$\langle \boldsymbol{f}, \boldsymbol{g} \rangle := \sum_{j=1}^{p} \int_{\mathcal{T}} f_j(t) g_j(t) dt,$$

where $\mathbf{f} = (f_1, \dots, f_p)^T$ and $\mathbf{g} = (g_1, \dots, g_p)^T$ in \mathbb{H} . The MFPCA identifies the eigenvalues and eigenfunctions that satisfy the spectral analysis of the covariance operator C. Specifically, we define the covariance operator $C : \mathbb{H} \to \mathbb{H}$ on $\mathbf{f} = (f_1, \dots, f_p)^T \in \mathbb{H}$ as

$$(Cf)^{i}(t) = \sum_{j=1}^{p} \int_{\mathcal{T}} V_{ij}(s,t) f_{j}(s) ds,$$

where $V_{ij}(s,t)$ is the (i,j)th element of $\boldsymbol{V}(s,t)$. Then, by the Hilbert–Schmidt theorem (Renardy, 2006), there exists a complete orthogonal basis of eigenfunctions $\boldsymbol{\psi}_r = (\psi_1^r, \dots, \psi_p^r)^T \in \mathbb{H}$ satisfying

$$C\psi_r = \lambda_r \psi_r$$
, for all $r = 1, 2, \dots$

and $\lambda_r \to 0$ as $r \to \infty$. Furthermore, the multivariate Karhunen–Lõeve expansion of $\boldsymbol{Z}(t)$ is

$$\boldsymbol{Z}(t) = \boldsymbol{\mu}(t) + \sum_{r=1}^{\infty} \xi_r \boldsymbol{\psi}_r(t),$$

where $\xi_r := \langle \mathbf{Z} - \boldsymbol{\mu}, \boldsymbol{\psi}_r \rangle$ is the rth functional principal component score. For N observations, the multivariate Karhunen–Lòeve expansion of $\mathbf{Z}_i(t)$ is

$$Z_i(t) = \mu_i(t) + \sum_{r=1}^{\infty} \xi_{ir} \psi_r(t) \text{ for } i = 1, \dots, N.$$

The functional principal component (FPC) scores $(\xi_{i1}, \xi_{i2}, \dots, \xi_{iR})^T$ are computed as $\xi_{ir} := \langle \mathbf{Z}_i - \boldsymbol{\mu}_i, \boldsymbol{\psi}_r \rangle$, where the number of FPCs, R is determined by the proportion of the explained variance.

Finally, we apply an existing clustering method, such as K-means algorithm and PAM algorithm, to the FPC scores of each day.

4 Real Data Analysis

4.1 Data and Setup

The step data used in this analysis are recorded for 21394 days over 79 people, with the number of days per person varying from 32 to 364. Our goal is to cluster 21394 days based on the amount, intensity, and pattern of activity. The current study focuses on clustering days, but the proposed method is readily applicable to clustering days for specific individuals with sufficient data. It can also be used to cluster individuals instead of days by connecting the daily step data from each subject as a single time series. Indeed, Section 4.4 discusses briefly clustering 79 individuals by the proposed method.

To construct the variables, we set the number of quantiles $Q_1 = 8$ for the ordered slope function $I_{Q_1}(t)$ that is suitable to reflect intense activity, such as exercise. For the mean score function, we use $P_{Q_2}(t)$ with $Q_2 = 4$, for grouping 24-hour activity patterns: early morning (0:00-6:00), morning (6:00-12:00), afternoon (12:00-18:00), and evening (18:00-24:00). For analysis, we obtain standardized functional data, $\{Z_{ki}(t)\}_{i=1,\ldots,N}$, $t=0,\ldots,T$, k=1,2,3, where N is the number of days (N=21394), and T=1440. Note that t=0 and t=1440 correspond to 12:00 AM.

Finally, the number of FPC scores in the MFPC procedure is selected using the total explained variance. This analysis uses the four leading MFPC scores that describe 92.97% of the total variance. Figure 6 shows the four leading estimated eigenfunctions for each variable. The first two eigenfunctions of the cumulative summation function, $\psi_1^1(t)$ and $\psi_1^2(t)$ are contrasted with each other for 07:00-17:00, while the first three eigenfunctions of the ordered quantile slope function, $\psi_2^1(t), \psi_2^2(t)$, and $\psi_2^3(t)$ look similar. Significantly different patterns in eigenfunctions of mean score

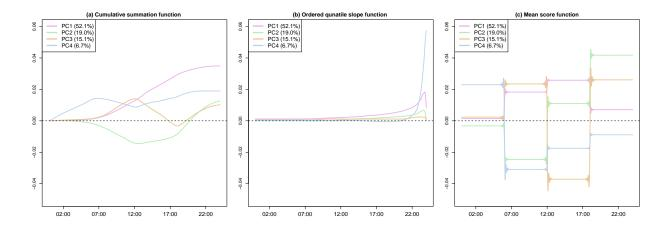


Figure 6: Estimates of the four eigenfunctions for each variable; $\psi_1^r(t)$ (left), $\psi_2^r(t)$ (middle), and $\psi_3^r(t)$ (right), for r = 1, 2, 3, 4 from multivariate FPCA. The number in parenthesis indicates the percentage of the explained variance.

function are observed.

As for the conventional clustering method applied to the MFPC scores, we use K-means and PAM algorithms.

4.2 Clustering Results

We apply the K-means algorithm to the MFPC scores and divide the total of 21394 days into seven subgroups. Note that for determination of an optimal number of clusters of K-means algorithm and PAM algorithm, we use the gap statistic (Tibshirani et al., 2001), which yields K = 7.

Figure 7(a) shows the mean curve of the step data in each group. The number in parenthesis in the figure indicates the number of days belonging to each group. We make some observations: (i) Cluster 6 is identified as the lowest-quantity and lowest-intensity group. (ii) The activities in Clusters 4 and 7 appear to be concentrated in the morning, although there are some differences in the amount of activity. (iii) Clusters 1 and 5 represent activities in the afternoon, although there is more significant activity in the former than in the latter. (iv) The days belonging to Cluster 3 show active movements in the evening. (v) Finally, the days in Cluster 2 tend to be relatively constant from morning to evening, but slightly more likely during rush hour.

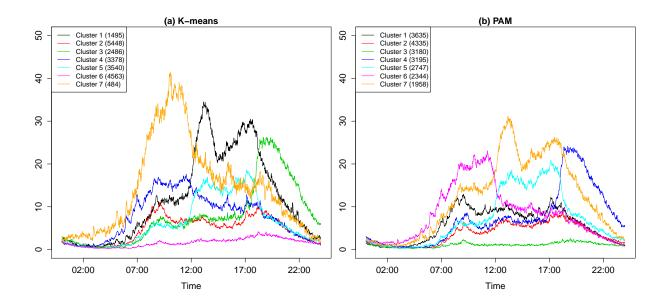


Figure 7: Mean curve of step counts in each group obtained from K-means and PAM. The number in parenthesis indicates the number of days in each group.

The heatmaps of the clustering results are shown in Figure 8 according to weekdays and weekends, indicating the proportion of days that an individual belongs to each cluster. Most individuals fall into Cluster 2 on weekdays, a group active during rush hour. Clusters 4 and 6 also include some individuals on weekdays that represent intermediate and minimum activity groups. On the other hand, most individuals belong to Cluster 6 on weekends, the minimum active group.

We now use the PAM algorithm to implement the proposed method for clustering the step data. The results are shown in Figure 7(b). We make some observations: (i) Clusters 3 and 7 are identified as the lowest- and the highest-quantity groups, respectively. In particular, the activities in Cluster 7 appear to be active from morning to afternoon. (ii) Cluster 4, as an intermediate-quantity group, is particularly active in the evening (18:00-24:00). (iii) The days belonging to Cluster 5 look brisk in the afternoon (12:00-18:00). (iv) The days in Cluster 6 show a lot of movement in the morning (06:00-12:00).

Compared with the results from the K-means algorithm, the days in each cluster are evenly distributed when using the PAM algorithm. It might be because the latter is more robust than the

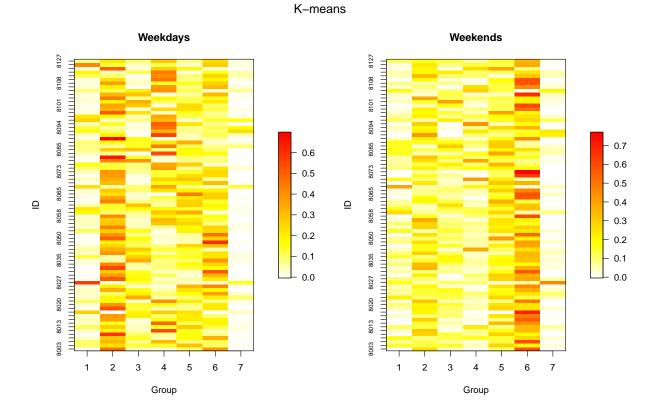


Figure 8: Heatmaps of clustering results from the proposed algorithm on weekdays and weekends.

The color code indicates the proportion of days that an individual belongs to each cluster.

former.

For visual assessment for clustering results, we randomly select a single day from each cluster obtained by the PAM algorithm. The corresponding cumulative sum functions, ordered quantile slope functions, and mean score functions are shown in Figure 9. From Figure 9(a), the amount of activities varies from cluster to cluster: the highest quantity group (Cluster 7), the mid-high quantity group (Clusters 4,5,6), the low-mid quantity group (Clusters 1,2), and the lowest quantity group (Cluster 3). Figure 9(b) shows that the highest intensity is observed in Cluster 7, the middle intensity for Clusters 2,4,5,6, and the low intensity group for Clusters 1,3. Finally, the pattern of activities is revealed from Figure 9(c) showing the average score function: the days in Clusters 1 and 6 prefer to walk in the morning (06:00-12:00), the days that belong to Clusters 2, 5, and 7 are active in the afternoon (12:00-18:00), and the movements of days in Cluster 4 are concentrated in

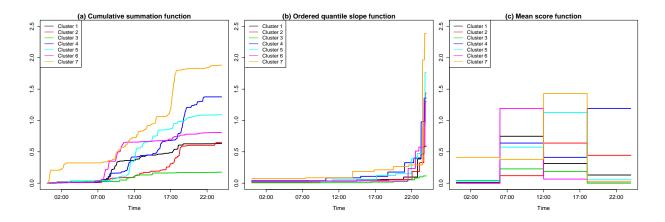


Figure 9: (a) Cumulative sum functions S(t), (b) ordered quantile slope functions $I_{Q_1}(t)$ with $Q_1 = 8$, and (c) mean score functions $P_{Q_2}(t)$ with $Q_2 = 4$ in each cluster obtained from PAM. the evening (18:00-24:00).

For further comparison, we apply the K-means and PAM algorithms directly to the raw step data. Figure 10 shows the mean curve of each cluster obtained by two algorithms. It is observed that for K-mean algorithms, 70.6% of the entire days are in Clusters 2 and 6, and for PAM algorithms, there are 88.2% in Clusters 1. Since more than 70% of days are clustered within a few groups, the mean curve of these groups seems flat due to the masking effect. On the other hand, from the results by the proposed method shown in Figure 7, we observe that days tend to be evenly distributed across clusters. We also find it difficult to observe the difference between the amount and intensity of the two clusters, although the patterns of the remaining clusters are different.

The proposed three input variables, S(t), $I_{Q_1}(t)$, $P_{Q_2}(t)$, can be used alone for K-means without MFPCA step, similar to Lim et al. (2019). Figure 11 presents the clustering results by applying K-means to each input variable. As expected, the K-means with the cumulative summation function, S(t), clusters the data according to the amount of the activity, and the result based on the mean score function, $P_{Q_2}(t)$, only reflects the pattern of the activity. We observe that the MFPCA step of the proposed method is necessary to simultaneously consider the amount, intensity, and pattern of the step data for clustering.

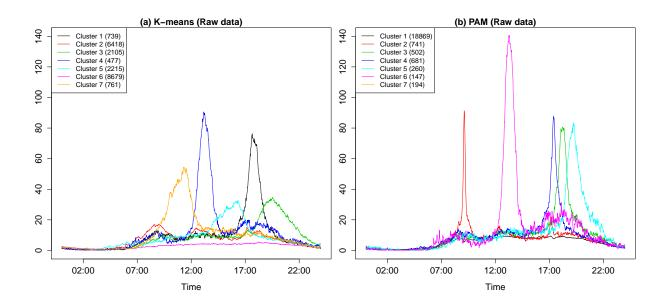


Figure 10: Mean curve of step counts in each cluster obtained from (a) K-means and (b) PAM applied to the raw step data directly.

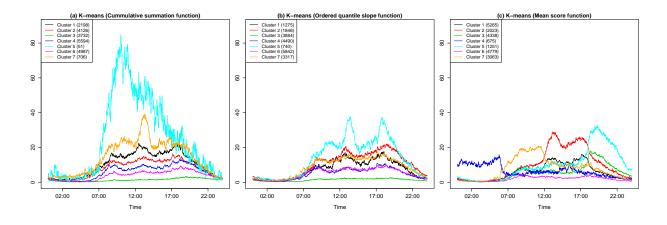


Figure 11: Mean curve of step counts in each cluster obtained from K-means only using (a) the cumulative summation function, (b) the ordered quantile slope function and (c) the mean score function.

4.3 Sensitivity Test for Q_1 of Ordered Quantile Slope Function

Unlike the Q_2 of the mean score function $P_{Q_2}(t)$ that can be easily set according to the time zone, it may seem quite difficult and arbitrary to select an optimal number of quantiles Q_1 of the ordered quantity function $I_{Q_1}(t)$. In addition, we observe from Figure 4 that $I_{Q_1}(t)$ varies with the choice of Q_1 value. Here we perform a sensitivity test with varying values of Q_1 . Note that the number of clusters is set to four, K=4. Figure 12 shows the heatmap image of clustering results obtained by PAM with $Q_1=4,6,8,12$. It seems that the clustering result is consistent with Q_1 values, indicating that the proposed method is not sensitive to the number of quantiles for the ordered quantile slope function.

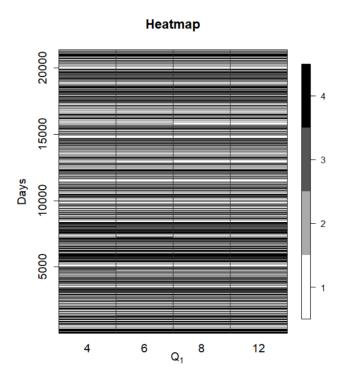


Figure 12: Heatmap of clustering results obtained by the proposed method with PAM. The color code indicates the cluster groups.

5 Simulation Study

5.1 Experimental Setup

To evaluate the empirical performance of the proposed method, we generate several simulated curves with different amounts, intensities, and patterns of activity.

Curves with different amounts

• Step-like simulation data: One important feature of step data is zero-inflation. From the real step data in Section 4, we observe that, out of 1440 minutes, the low amount group is active for about 150 minutes, the middle amount group for about 250 minutes and the high amount group for about 350 minutes. Therefore, we generate the number of non-zero points in the *i*th curve for the *k*th group as follows:

$$N_{i,k} = \lfloor W \rfloor, \quad W \sim N(\mu_k, \sigma^2), \quad i = 1, ..., n_k, \quad k = 1, 2, 3,$$

where $(\mu_1, \mu_2, \mu_3) = (150, 250, 350)$, $\sigma^2 = 15$, and $N := \sum_k n_k$. Here, $\lfloor x \rfloor$ denotes the largest integer less than or equal to x. Then, the ith simulated step data in group k, $Y_{i,k}(t)$, has a nonzero value at $t \in \mathbb{T}_{i,k}$, where the number of time points in $\mathbb{T}_{i,k}$ is $N_{i,k}$. To fix the intensity and pattern for all curves $(i = 1, \dots, N)$, we set $\mathbb{T}_{i,k}$ as follows: 75% of $\mathbb{T}_{i,k}$ are randomly located in $t = 481, \dots, 960$, and 21% of $\mathbb{T}_{i,k}$ are in $t = 241, \dots, 480, 961, \dots, 1200$. The remaining 4% are in $t = 1, \dots, 240$ and $t = 1201, \dots, 1440$. Now, the tth simulated step data in group t is generated from the following exponential distribution,

$$Y_{i,k}(t) = \begin{cases} \lfloor Z \rfloor, & Z \sim \text{Exp}(1/\lambda), & t \in \mathbb{T}_{i,k}, \\ 0, & t \notin \mathbb{T}_{i,k}, \end{cases}$$
 $i = 1, \dots, n_k, \quad k = 1, 2, 3,$ (2)

where $\lambda = 32.5$ that denotes the estimated overall mean of the real step data. We generate $n_k = 100, k = 1, 2, 3$, random curves from each group. Each realization of random curves according to groups is shown in the first row of Figure 13.

• Sinusoidal signal: We generate a random curve defined as

$$Y_{i,k}(t_j) = a_k \left| \sin(\frac{5t_j}{T}) + \varepsilon_{ijk} \right|, \quad j = 1, \dots, T, \ i = 1, \dots, n_k, \ k = 1, \dots, 4,$$
 (3)

where $t_j = \frac{j-1}{T}$ with T = 1024, and $\varepsilon_{ijk} \sim N(0, \sigma^2)$ with $\sigma^2 = 0.5$. Then, we set $\boldsymbol{a} = (a_1, a_2, a_3, a_4) = (1, 1.1, 1.2, 1.3)$ to reflect the difference in the amounts. Here we generate $n_k = 50$ random curves in each group. Sample curves from each group are shown in the second row of Figure 13.

Curves with different intensity

• Step-like simulation data: We generate $n_k = 100$ curves with different intensities according to three groups (k = 1, 2, 3). Similarly, the number of nonzero points in the *i*th curve for the kth group is generated as

$$N_{i,k} = \lfloor W \rfloor, \quad W \sim N(\mu, \sigma^2), \quad i = 1, \dots, n_k, \quad k = 1, 2, 3,$$
 (4)

where $\mu = 150$ and $\sigma^2 = 10$. Then, the *i*th simulated step data in group *k* have nonzero values at $t \in \mathbb{T}_{i,k}$, where the number of time points in $\mathbb{T}_{i,k}$ is $N_{i,k}$.

To further vary the intensities in the data, we define $\mathbb{T}_{i,k}$ differently for each group k. For the first group, we generate curves with low intensity as follows: 20% of $\mathbb{T}_{i,1}$ are randomly located in $t=1,\ldots,480$, and 30% and 50% of $\mathbb{T}_{i,1}$ are in $t=481,\ldots,960$ and $t=961,\ldots,1440$, respectively. For the second group, we define $\mathbb{T}_{i,2}$ with a narrower interval than that of $\mathbb{T}_{i,1}$: 20% of $\mathbb{T}_{i,2}$ are randomly located in one of two intervals, $t=1,\ldots,240$ or $t=241,\ldots,480$; 30% of $\mathbb{T}_{i,2}$ are randomly located in one of $t=481,\ldots,720$ and $t=721,\ldots,960$; and 50% of $\mathbb{T}_{i,2}$ are randomly located in small intervals in $t=961,\ldots,1440$. For the last group, we generate high-intensity curves: 20% of $\mathbb{T}_{i,3}$ are randomly located in one of the four intervals, $t=1,\ldots,120,\ t=121,\ldots,240,\ t=241,\ldots,360,\$ and $t=361,\ldots,480;\$ 30% of $\mathbb{T}_{i,3}$ are randomly located in one of the four intervals, $t=481,\ldots,600,\ t=601,\ldots,720,\$ $t=721,\ldots,840,\$ and $t=841,\ldots,960,\$ and 50% of $\mathbb{T}_{i,3}$ are densely located in small intervals

in $t = 961, \dots, 1440$. Now, the ith simulated step data in group k are defined as

$$Y_{i,k}(t) = \begin{cases} \lfloor Z \rfloor, & Z \sim \text{Exp}(1/\lambda), & t \in \mathbb{T}_{i,k}, \\ 0, & t \notin \mathbb{T}_{i,k}, \end{cases}$$
 $i = 1, \dots, n_k, \quad k = 1, 2, 3,$ (5)

where $\lambda = 20$. Three sample curves are shown in Figure 14.

Curves with different patterns

- Step-like simulation data: We generate $n_k = 100$ random curves with different patterns from three groups (k = 1, 2, 3). We generate $N_{i,k}$ as (4) with $\mu = 250$ and $\sigma^2 = 15$, and $Y_{i,k}(t)$ is generated as (5) with $\lambda = 32.5$. To have a different pattern for each group, we generate $\mathbb{T}_{i,k}$ differently for k = 1, 2, 3. For the first group (k = 1), 45% of $\mathbb{T}_{i,k}$ are randomly located in $t = 1, \ldots, 480$, and 35% and 20% of $\mathbb{T}_{i,k}$ are in $t = 481, \ldots, 960$ and $t = 961, \ldots, 1440$, respectively. For the second group (k = 2), 35% of $\mathbb{T}_{i,k}$ are randomly located in $t = 1, \ldots, 480$, and 45% and 20% of $\mathbb{T}_{i,k}$ are in $t = 481, \ldots, 960$ and $t = 961, \ldots, 1440$, respectively. For the last group (k = 3), the proportions are 20%, 35%, and 45%, respectively. Sample curves from each group are plotted in the first row of Figure 15.
- Shifted Doppler signal: We generate 50 random curves in four groups that have different patterns:

$$Y_{i,k}(t_j) = 0.6 + 0.6\sqrt{t_j(1-t_j)} \sin\left(\frac{2.1\pi}{t_j-t_{0,k}}\right) + \epsilon_{ijk}, \quad j=1,\ldots,T, \ i=1,\ldots,n_k, \ k=1,\ldots,4,$$
 where $t_j = \frac{j-1}{T}, \ T=512$ and $\epsilon_{ijk} \sim N(0,0.05^2)$. To have a different pattern for each group, we set the shift parameter $t_{0,k}=0,1/3,2/3,1$ for each k . Sample curves from each group are plotted in the last row in Figure 15.

We compare the proposed methods with two existing methods used for clustering multivariate functional data, FunFEM and FunHDDC.

- MFPCA-Kmeans: Proposed method with the K-means algorithm.
- MFPCA-PAM: Proposed method with the PAM algorithm.

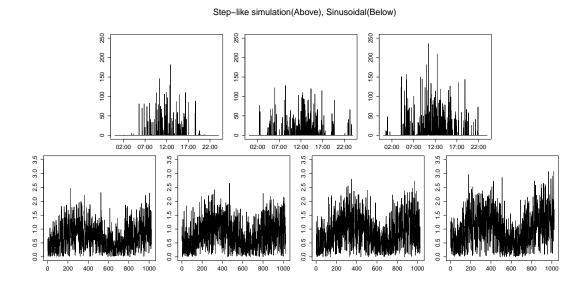


Figure 13: Simulated step-like data with different amounts (top row), and simulated sinusoidal curves with different amounts (bottom row).

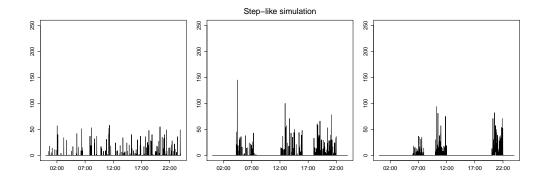


Figure 14: Sample step-like data with different intensity.

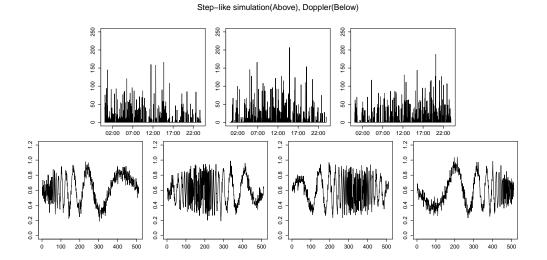


Figure 15: Sample step-like data with different patterns (top), and sample doppler curves with different patterns (bottom).

- FunFEM: Functional clustering based on discriminative functional mixture modeling of Bouveyron et al. (2016).
- FunHDDC: Functional clustering based on functional latent mixture modeling of Schmutz et al. (2020).

For the proposed methods, we set the number of quantiles for the ordered quantile slope function $I_{Q_1}(t)$ as $Q_1 = 8$ and the number of quantiles for the mean score function $P_{Q_2}(t)$ as $Q_2 = 4$.

5.2 Results

As for evaluation measure, we use the correct classification rate (CCR) (%) and the adjusted Rand index (aRand) of Hubert and Arabie (1985). Note that aRand is a corrected version of the Rand index (Rand, 1971) that measures the correspondence between two partitions classifying the object pairs in a contingency table. It further adjusts the Rand index to have an expected value of zero with an upper bound. Thus, a larger aRand value indicates a higher similarity between the two partitions.

The CCR (%) and aRand values over 100 simulations are listed in Table 1. We have some observations: (i) The proposed methods work well in almost every case. (ii) For the curves with different amounts, the proposed methods outperform two existing methods. (iii) The proposed MFPCA-PAM outperforms for clustering curves with different patterns. (iv) For the intensity cases, the MFPCA-PAM provides the best results.

6 Conclusion

In this paper, a new clustering method is proposed for discrete, high-dimensional, and zero-inflated step data. We introduce new variables that reflect the unique characteristics of the data while maintaining important information from the original data. By applying the MFPCA-based method to the new variables, we can simultaneously account for the multiple features—amount, intensity, and pattern—of step data in the clustering algorithm. Through numerical experiments involving a simulation study and real data analysis, the proposed method shows efficient clustering performance of various functional data, including step count data. We believe that our study contributes to the literature by greatly expanding the range of multivariate function data clustering. Finally, it is necessary to determine some parameters, such as the optimal number of quantiles Q, to implement the proposed method. It is left for future work.

References

Balli, S., Sağbas, E. A. and Hokimoto, T. (2017). The usage of statistical learning methods on wearable devices and a case study: activity recognition on smartwatches. *Advances in Statistical Methodologies and Their Application to Real Problems*, InTech Press, Rijeka, 259–277.

Bassett Jr, D. R., Wyatt, H. R., Thompson, H., Peters, J. C. and Hill, J. O. (2010). Pedometer-measured physical activity and health behaviors in United States adults. *Medicine & Science in Sports & Exercise*, **42**, 1819.

Table 1: Means and standard deviations (in parentheses) of the correct classification rate (CCR) and adjusted rand index (aRand) values.

test function	k	CCR			
		MFPCA-Kmeans	MFPCA-PAM	FunFEM	FunHDDC
Amount					
Step simulation	3	0.9911 (0.005)	0.9914 (0.006)	0.6440 (0.026)	0.6210 (0.083)
Sinusoidal	4	$0.9225 \ (0.134)$	0.9613 (0.016)	$0.6312\ (0.073)$	0.9347 (0.117)
Pattern					
Step simulation	3	$0.8636 \ (0.215)$	0.9944 (0.003)	0.7279 (0.046)	0.7158 (0.101)
Doppler	4	0.8244 (0.184)	0.9767 (0.010)	1 (0)	0.8269 (0.171)
Intensity					
Step simulation	3	$0.6298\ (0.037)$	$0.6021 \ (0.052)$	$0.5972\ (0.070)$	$0.5993 \ (0.075)$
test function	k	aRand			
		MFPCA-Kmeans	MFPCA-PAM	FunFEM	FunHDDC
Amount					
Step simulation	3	$0.9735 \ (0.016)$	$0.9743\ (0.016)$	0.3826 (0.041)	0.3428 (0.1277)
Sinusoidal	4	0.8825 (0.161)	0.9008 (0.040)	0.4415 (0.063)	$0.8985 \ (0.129)$
Pattern					
Step simulation	3	$0.8397 \ (0.252)$	0.9832 (0.010)	0.4881 (0.077)	$0.5472\ (0.086)$
Doppler	4	0.7956 (0.187)	$0.9405 \ (0.025)$	1 (0)	0.8105 (0.188)
Intensity					
Step simulation	3	$0.3440\ (0.054)$	$0.2548 \; (0.079)$	$0.2796 \ (0.1225)$	0.2886 (0.1276)

- Bouveyron, C., Come, E. and Jacques, J. (2016). The discriminative functional mixture model for the analysis of bike sharing systems. *Annals of Applied Statistics*, **9**, 1726–1760.
- Cheung, Y. K., Hsueh, P. Y. S., Ensari, I., Willey, J. Z., and Diaz, K. M. (2018). Quantile coarsening analysis of high-volume wearable activity data in a longitudinal observational study. *Sensors*, **18**, 3056.
- Chiou, J. M. and Li, P. L. (2007). Functional clustering and identifying substructures of longitudinal data. *Journal of the Royal Statistical Society Series B*, **69**, 679–699.
- Chiou, J. M., Chen, Y. T. and Yang, Y. F. (2014). Multivariate functional principal component analysis: A normalization approach. *Statistica Sinica*, **24**, 1571–1596.
- de Boor, C. (1978). A Practical Guide to Splines. Springer-Verlag, New York.
- Hubert, L. and Arabie, P. Comparing partitions. (1985). Comparing partitions. Journal of Classification, 2, 193–218.
- Jacques, J. and Preda, C. (2014). Model-based clustering for multivariate functional data. *Computational Statistics and Data Analysis*, **71**, 92–106.
- Kaufman, L. and Rousseeuw, P.J. (1987). Clustering by means of medoids. Statistical Data Analysis

 Based on the L₁-Norm and Related Methods, North-Holland, 405–416.
- Kaufman, L. and Rousseeuw, P. (1990). Finding Groups in Data: An Introduction to Cluster Analysis. Wiley, New York.
- Le Masurier, G.C., Beighle, A., Corbin, C.B., Darst, P.W., Morgan, C., Pangrazi, R.P., Wilde, B. and Vincent, S.D. (2005). Pedometer-determined physical activity levels of youth. *Journal of Physical Activity and Health*, 2, 159–168.
- Lim, Y., Oh, H.-S. and Cheung, K. (2019). Functional clustering of accelerometer data via transformed input variables. *Journal of the Royal Statistical Society Series C*, **68**, 495-520.

- Ramsay, J.O. and Silverman, B.W. (2005). Functional Data Analysis, Second edition. Springer, New York.
- Rand, W. M. (1971). Objective criteria for the evaluation of clustering methods. *Journal of the American Statistical Association*, **66**, 846–850.
- Renardy, M. and Rogers, R. C. (2006). An Introduction to Partial Differential Equations, Springer, New York.
- Schmutz, A., Jacques, J., Bouveyron, C., Cheze, L. and Martin, P. (2020). Clustering multivariate functional data in group-specific functional subspaces. *Advances in Data Analysis and Classification*, In Press.
- Shoaib, M., Bosch, S., Incel, O., Scholten, H. and Havinga, P. (2015). A survey of online activity recognition using mobile phones. *Sensors*, **15**, 2059–2085.
- Tibshirani, R., Walther, G. and Hastie, T. (2001). Estimating the number of clusters in a data set via the gap statistic. *Journal of the Royal Statistical Society Series B*, **63**, 411–423.